Analyzing Velocity Structure and Scattering in Homestake Area

Zhi Li[1], Gabriel Gribler[2], Lee M. Liberty[2], Daniel C. Bowden[3], Victor C. Tsai[3]

[1]School of Earth and Space Sciences, University of Science and Technology of China

[2]Department of Geosciences, Boise State University

[3]Seismological Laboratory, California Institute of Technology, Pasadena

lizhi555@mail.ustc.edu.cn

Abstract. *An array of broadband seismometers with 3D geometry has been deployed at the former Homestake Mine in South Dakota to study the underground seismic field and noise. This data has provided us a good chance to understand how wavefield varies with depth and to improve teleseismic earthquake signals. To analyze the influence of shallow structure on wavefield, weight drop experiment has been conducted to determine the shallow velocity distribution. With the active source data, we invert for both P wave and S wave velocity structure: P wave inversion with wavepath eikonal traveltime method; S wave inversion with a joint-inversion method for Rayleigh-wave dispersion and horizontal-to-vertical (H/V) spectral ratios. To analyze the influence of near-surface scattering on teleseismic signals, fk analysis has been applied to a teleseismic earthquake in Japan. We compare the result of fk analysis at different frequency ranges, in different depths, and show that (1) the "deep" stations (4000's) have a more coherent signal than the "shallow" stations (0-300), (2) station geometry have an influence on the shape of the fk peak, but roughness of the fk plot is due to the data, (3) higher frequency range we stack, the incoherent the fk plot looks, (4) limitation of the station number and distribution makes it hard to identify how the incoherence varies with space. This result seems to be consistent with near-surface scattering and potentially indicates that complexity decreases with depth.*

Keywords*: Homestake Mine, Active Source, Near-surface scatteing, fk analysis.*

1. Background

For next generation of LIGO, which aims to probe the gravitational waves with a lower frequency, how to identify the signals from the universe with those caused by the seismic event or density fluctuations (Newtonian noise) is the foremost challenge to guarantee the sensitivity of the observation [Harms et al. 2009]. This motivated the seismic study of the former Homestake mine in Lead, South Dakota, a very promising candidate site. It is being transformed gradually into a scientific laboratory which now is known as the Sanford Laboratory. It lies far from the oceans and has the deepest reaching tunnels in North America (8000 ft) which provides an optimal stage for monitoring the seismic signals with a three dimensional network of seismometers.

In recent two years, the experiments in Homestake cooperated by several research

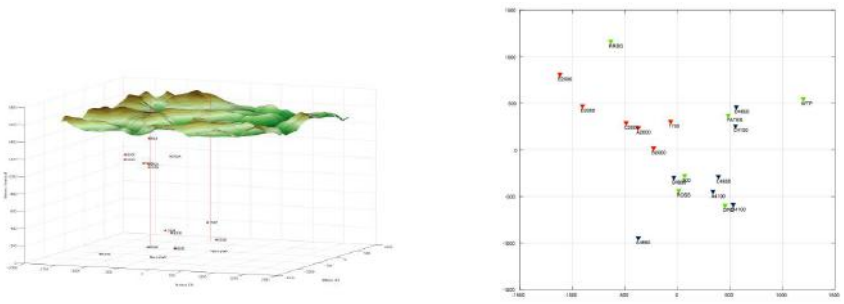

(a) 3D view (b) Plane view

Figure 1. Seismometer distribution. [Color code: Deep(black), Middle(red), Surface(green)]

groups have constantly provided unprecedented data in different depth, much wider than normal boreholes, for researchers to shed light on the wave propagation in shallow structure (Figure1). Also, the complex geology at Homestake has made it an ideal place to study the seismic wave propagation through layers with strong lateral heterogeneity, attenuation, scattering and interaction with free surface.

Variations and fluctuations caused by lateral heterogeneity in near surface always bring great difficulties to seismologists who want to make use of the signals from distant and deep sources (e.g. back projection). Accordingly, how to analyze the noise or irregular, messy signals mostly due to the shallow structure and make corrections of these signals is a challenging problem we are interested in.

2. Analyzing the velocity structure of Homestake area

Figure 2. Surface shot plan

To determine the tomography of this region, it is extremely important to obtain the very near-surface velocity structure because it would provide the vital and accurate restraint on the deeper research. The signals collected by seismometers distributed underground are strongly affected by the regional factors around the monitors. Any inaccurate observation may bring uncertain variations or errors to the further research. These motivated our design of an active source survey. We use the weight-drop hammer as the source and

record the seismic signals via a land streamline device. The field work has finished. With the active source data, we do both P-wave and S-wave inversion.

2.1. P wave inversion

A standard refraction processing flow would be undertaken to develop the P wave structure from the first shock arrival time. The method is based on wavepath eikonal traveltime inversion, which computes wavepaths by using finite-difference solutions to the eikonal equation. In this inversion, the velocity model is updated by iteratively back-projecting the traveltime residuals along rays. And it focuses more on fat-ray or Fresnel-volume tomography. The below is part of the result:

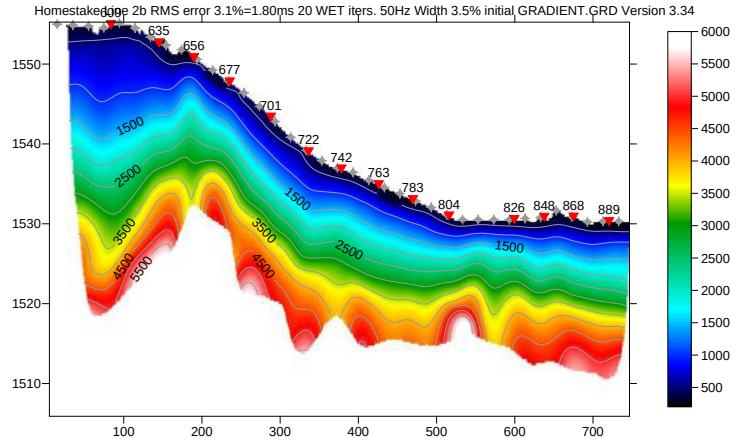

(a) Kirk Road Profile

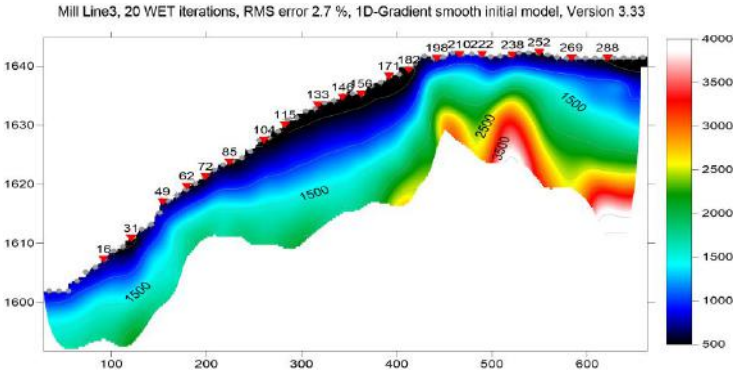

(b) Mill Road Profile

Figure 3. P wave tomography

Our result (Figure 3) shows P-wave velocity structure in shallow Homestake area is quite complex. We observe the twisted bedrock underneath the sediment layer. The result shows good agreement with the surface tomography. These can be a good reference to S-wave inversion.

2.2. S wave inversion

For surface wave, we present a joint-inversion method for Rayleigh-wave dispersion and horizontal-to-vertical (H/V) spectral ratios. Incorporating the H/V data adds additional information to the inversion and improves the near-surface shear wave velocity distri-

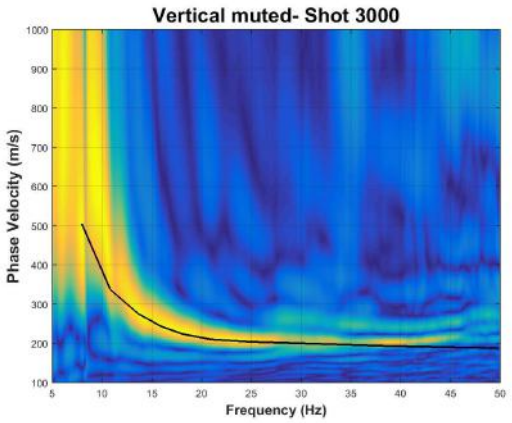

Figure 4. Extracting dispersion curve1

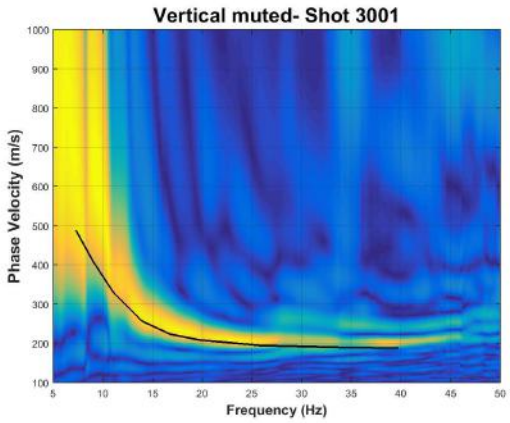

Figure 5. Extracting dispersion curve 2

bution in shallow hard-rock environments. Our active source joint-inversion approach is able to accurately estimate shear wave velocity distributions when Rayleigh-wave dispersion inversion alone fails. We use multi-offset multi-component active source seismic data recorded on vertical and horizontal in-line geophones.

From these data we generate an H/V curve and estimate Rayleigh-wave phase velocities. We employ the genetic algorithm to jointly invert these separate data sets and estimate the shear-wave velocity distribution as a function of depth.
The figure below shows part of our result of S wave inversion:

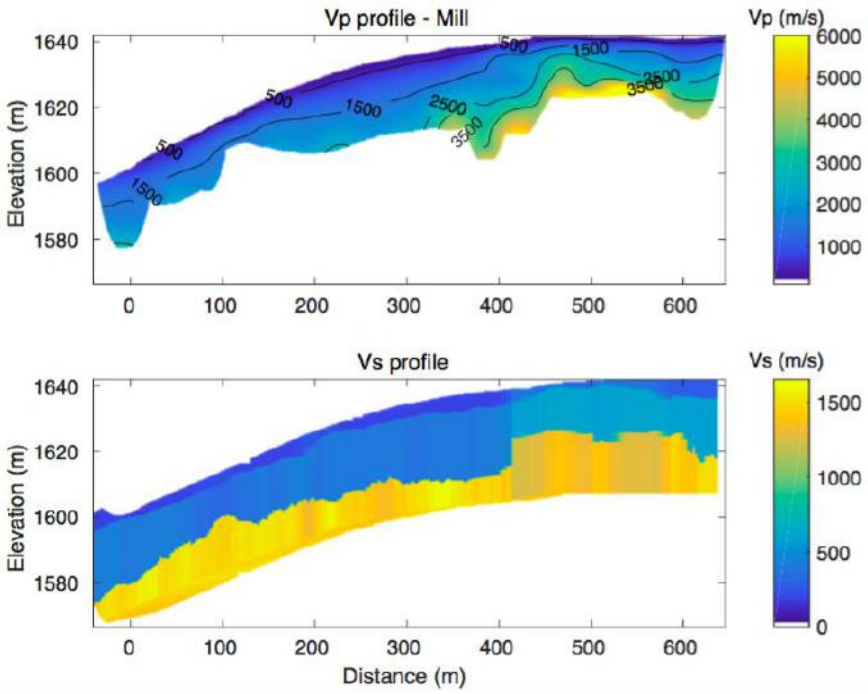

Figure 6. P wave and S wave velocity profile of Mill Road

Our result (Figure 6 and Figure 7) shows S wave velocity profile agrees very well with the P wave velocity profile.

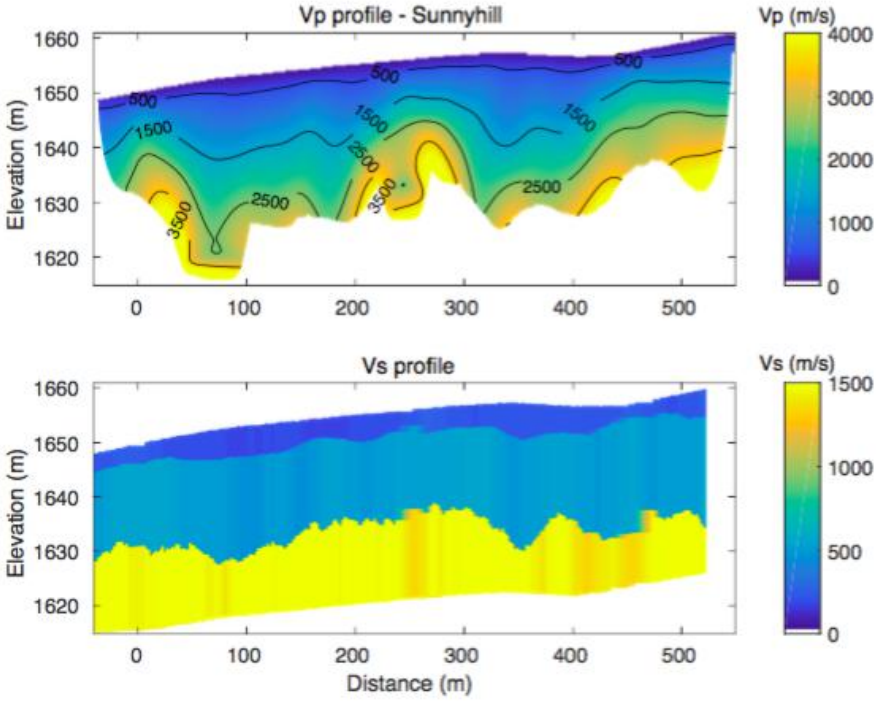

Figure 7. P wave and S wave velocity profile of Sunnyhill Street

3. Analyzing the scattering in Homestake area

[Spudich and Bostwick 1987] and [Scherbaum et al. 1991] first showed that the early S coda was dominated by multiple scattering within the shallow structure, using the the virtual seismic array (source array) deep underground with the reciprocity of the Green's function [Shearer 2007]. However, such result is doubted because the accuracy of the results depends, to a great extent, on the quality of the available information about the sources, such as location, origin times, and source mechanism [Rost and Thomas 2002]. The data collected in the 3D Homestake array do not need to use the reciprocity, thus they could provide directly the first-hand information to identify the strong scattering in the shallow layer (areas above the deepest stations).

3.1. Method

One way to find the propagation direction of component waves using array observations is to use a frequency-wavenumber power spectrum, also known as fk analysis [Sato et al. 2012]. The frequency–wavenumber analysis (fk analysis) is able to measure the complete slowness vector (i.e. back azimuth and horizontal slowness) simultaneously. The fk analysis calculates the power distributed among different slownesses and directions of approach. The time delays required to bring the signals into phase provide a direct estimate of the back azimuth and the slowness of the signal. When the slowness and back azimuth of a signal are unknown, a grid search for all u and combinations can be performed to find the best parameter combination, producing the highest amplitudes of the summed signal. This computation is performed in the spectral domain to save computation time.

Derivations for fk analysis

Assume a signal arriving at a reference point within the array with a horizontal velocity v_s and a back azimuth is described as $s(t)$. The nth seismometer with the location vector $\mathbf{r_n}$, relative to the array reference point records the signal $x_n(t)$:

$$x_n(t) = s(t - \mathbf{u} \cdot \mathbf{r_n})$$

where $\mathbf{u}$ is the slowness vector.
Then from the record of the array, we can derive the signal at the reference point:

$$y(t) = \frac{1}{N} \sum_{n=1}^{N} x_n(t + \mathbf{u} \cdot \mathbf{r_n})$$

we can calculate the erergy distribution as a function of $\mathbf{u}$ in frequency domain.
Using Parseval's Theorem, the total energy recorded at the array can be calculated by the integration of the squared summed amplitudes over time:

$$E = \int_{-\infty}^{\infty} |y(t)|^2 dt = \int_{-\infty}^{\infty} |Y(f)|^2 df$$

where $Y(f) = \mathcal{F}\{y(t)\}$.
For DFT, the form is:

$$\sum_{n=0}^{N-1} |x[n]|^2 = \frac{1}{N} \sum_{k=0}^{N-1} |X[k]|^2$$

Thus,

$$Y(f) = \int_{-\infty}^{\infty} y(t) e^{-i2\pi f t} dt = \frac{1}{N} \sum_{n=1}^{N} \int x_n(t + \mathbf{u} \cdot \mathbf{r_n}) e^{-i2\pi f t} dt$$
$$= \frac{1}{N} \sum_{n=1}^{N} X_n(f) e^{i2\pi f \mathbf{u} \cdot \mathbf{r_n}}$$

$$E = \int_{-\infty}^{\infty} |y(t)|^2 dt = \int_{-\infty}^{\infty} |Y(f)|^2 df$$
$$= \int_{-\infty}^{\infty} |\frac{1}{N} \sum_{n=1}^{N} X_n(f) e^{i2\pi f \mathbf{u} \cdot \mathbf{r_n}}|^2 df$$

So the result of fk analysis can be distributed as a function of slowness and back azimuth. Specifically, we call

$$|A(\mathbf{u})|^2 = |\frac{1}{N} \sum_{n=1}^{N} e^{i2\pi f \mathbf{u} \cdot \mathbf{r_n}}|^2 df$$

as the array response function (ARF)[Rost and Thomas 2002]. This array response function (ARF) directly reflects the delta impulse response of the array. The ARF is controlled by the design (aperture, configuration, and interstation spacing) of the array. The ARF of different station geometry is shown in Figure 8.

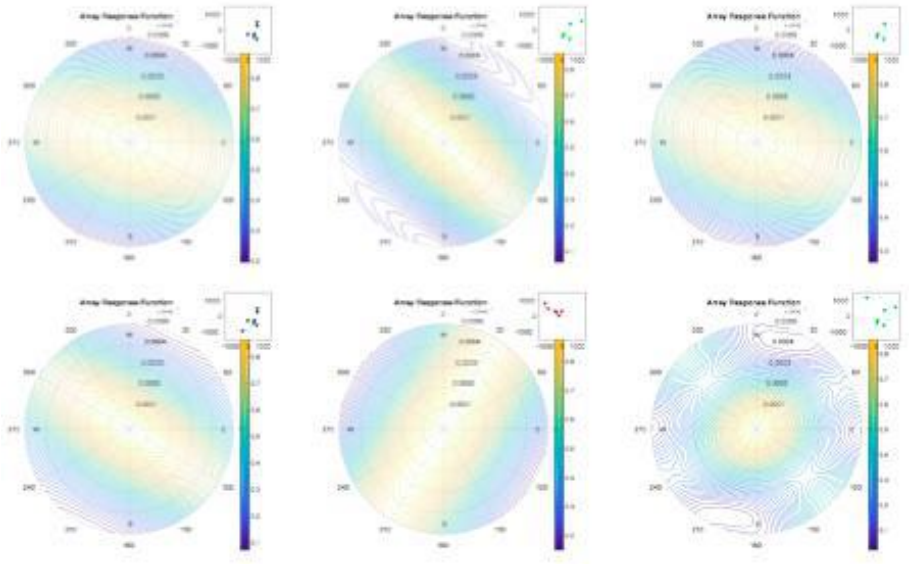

Figure 8. Array response function (ARF) of different station geometry.

3.2. Synthetic test of fk analysis

Figure 9 shows the frequency-wavenumber diagrams of different synthetic signals. The synthetic signals are composed of the real ambient noise, which is recorded one hour before the Japan earthquake, and a damped sine signal with different signal noise ratio (SNR) listed in the figure. The synthetic signals arrive with a slowness of 0.0003 s/m and along a backazimuth of 30°. The signal noise ratio are varied from 100% ($A_{signal}/A_{noise} = 1 = 100\%$) to 20% ($A_{signal}/A_{noise} = 1 = 20\%$). Our test shows the slowness and backazimuth are correctly resolved by the fk-analysis when the SNR is larger than 40%, however, the synthetic signal is buried in ambient noise when the SNR is around 20%.

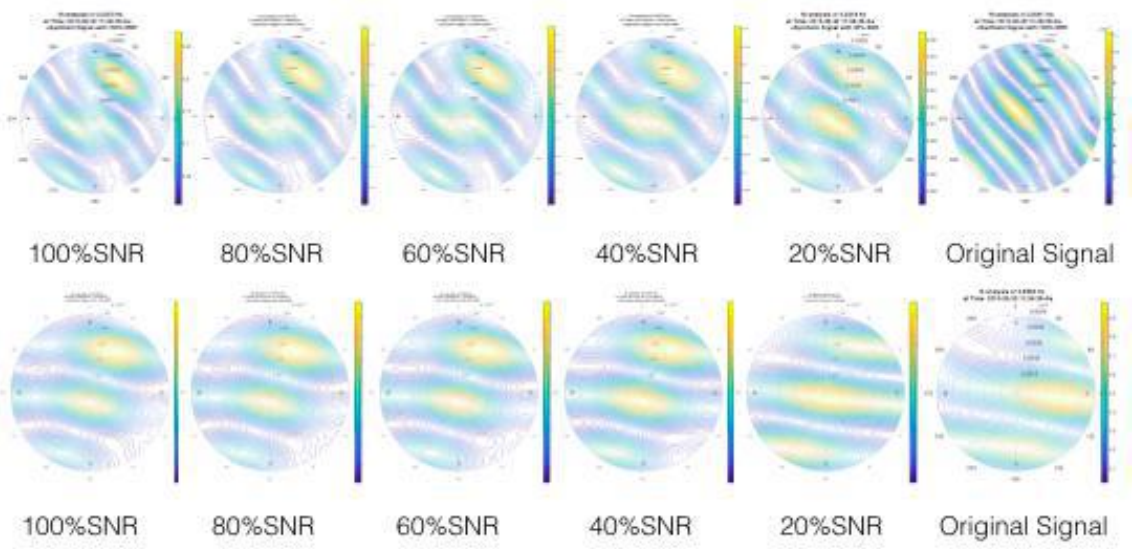

Figure 9. Examples of frequency-wavenumber diagrams (fk-diagrams) and noise resolution test for the fk-analysis. The real ambient noise is added to each synthetic signals.

3.3. Result of fk analysis

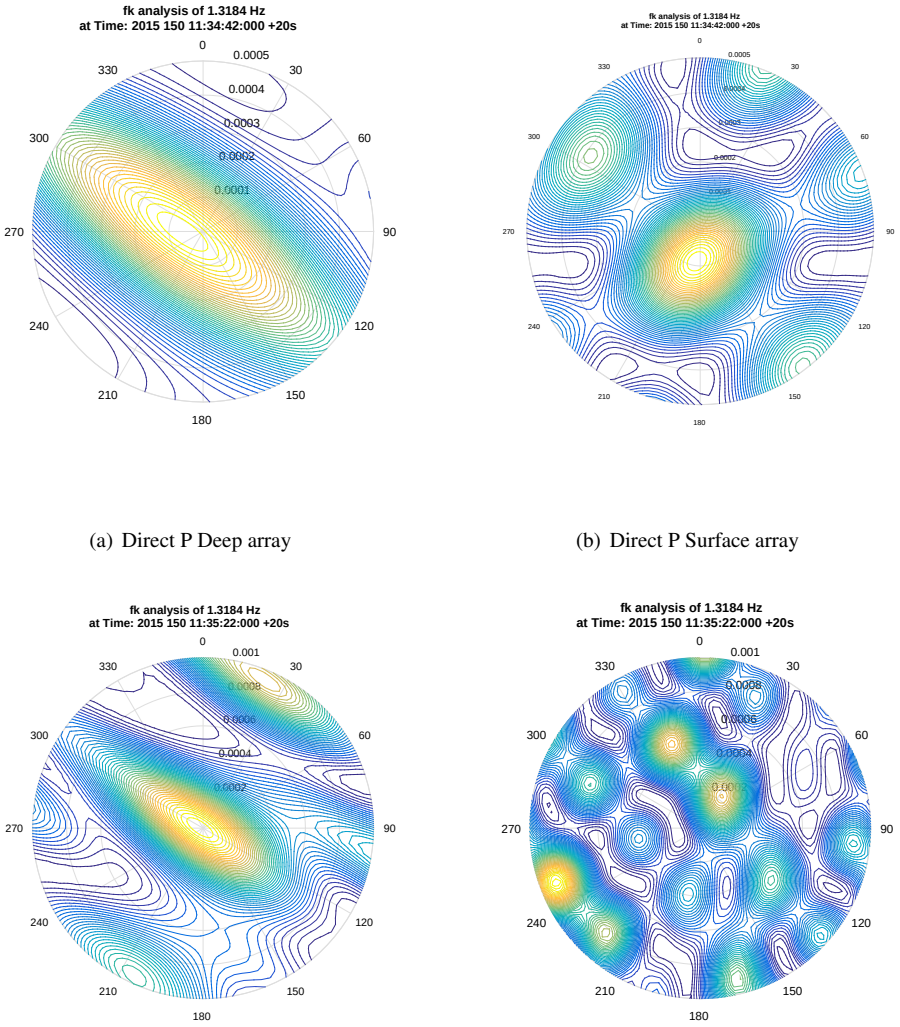

(a) Direct P Deep array

(b) Direct P Surface array

(c) P Coda Deep array

(d) P Coda Surface array

Figure 10. fk analysis of Japan Earthquake: The color in the plot means the power distribution. A peak indicates the direction of approach and the apparent propagation velocity of the plane wave that crosses the array. The analysis was performed with the raw data from 20 s time windows, one pair surrounding the direct P-arrival, and one pair beginning 40 s after the direct P-arrival.

For wavefield data having a finite duration in a given frequency band having center frequency f, we generate contour plots of the estimated fk power spectral density P_f in the horizontal slowness plane. We choose the highest signal within the given band as the center freqency f. Figure 10(a) shows results of an fk analysis of data recorded by 2 different seismic array, located at the deep and surface part in Homestake Mine of a Mw 7.7 earthquake in Japan. We compare the wave approaching direction at different level of depth. We show that, at deep array, the approaching wave have a certain direction (or intensed distribution Figure10(a),10(c)), while at the surface the waves are composed of wavelets in a variety of direction (Figure10(b),10(d)). The result suggests that the structure between the deep stations and the surface is the dominant factor that causes the variance.

Also, the peak being near the origin indicates that the apparent slowness $\mathbf{u}$ is small. The apparent slowness $\mathbf{u}$ is determined by v_0, the medium velocity beneath the array, and incident angel i:

$$u = \frac{1}{v_{app}} = \frac{\sin i}{v_0}$$

This shows either i is small, which means the incident waves is steep, or the medium velocity is very fast. This matches our expectation of the teleseismic event in Japan.

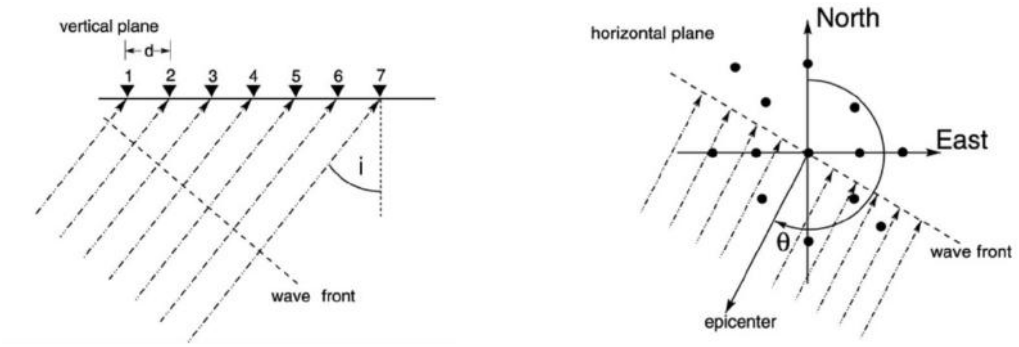

Figure 11. (a) The vertical plane of an incident wave front crossing an array at an angle of incidence i. (b) Sketch of the horizontal plane of an incident plane wave arriving with a back azimuth θ.

FK diagrams of P coda in a different frequency search range(Figure 12) shows a similar result of scattered pattern between surface array and deep array.

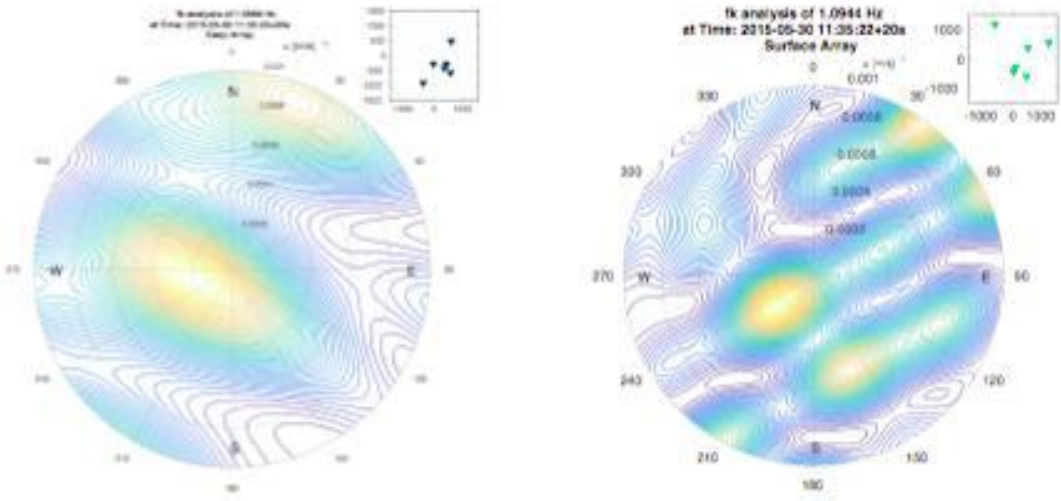

Figure 12. Other example of fk analysis of Japan Earthquake P coda in a different frequency range 1-1.5 Hz

3.4. Stacking of fk analysis

In previous fk analysis, we use the frequency components with the highest amplitude in a given frequency range to represent the strongest signal. It is also important to know the fk analysis result of all the frequency components. Figure 13 shows the whole energy distribution of all the frequency components. Clear difference between the result of surface array and deep array can also been seen.

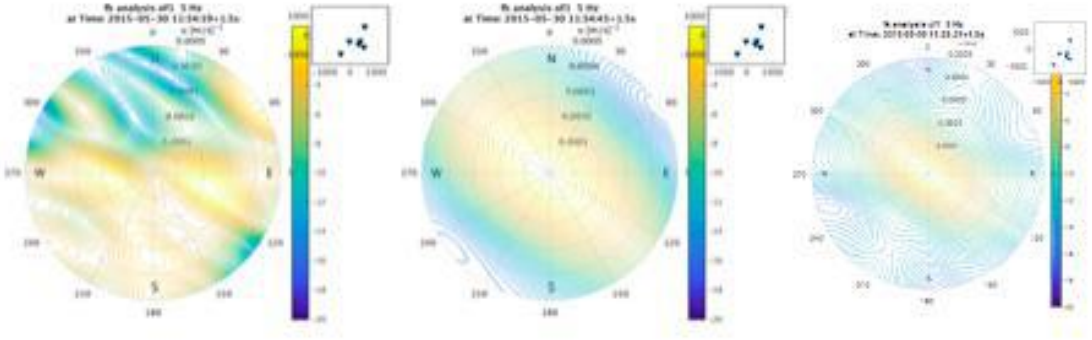

(a) Deep array stacking of ambient noise, first P, P coda (from left to right)

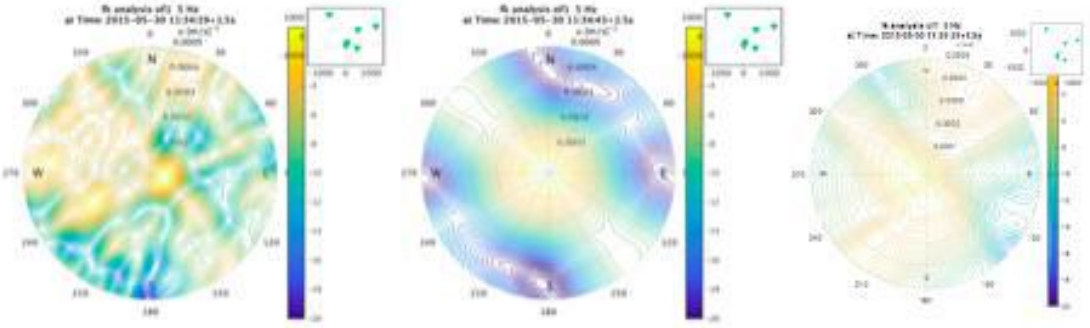

(b) Surface array stacking of ambient noise, first P, P coda (from left to right)

Figure 13. fk diagrams stacking of all the frequency components

4. Discussion

4.1. Determining the time window

The accuracy and resolution of the method is greatly influenced by the choosing time window. The width of the window relates to how the signal is represented—A wide window gives better frequency resolution but poor time resolution, thus may contain several different phases that makes the plot ambiguous. A narrower window gives good time resolution but poor frequency resolution which may change the result of the fk analysis.

The cause of the problem is that the earthquake signals is normally non-stationary signals. In this cases, the direct Fourier transform(fft,dft), widely used in many papers and codes, would be not enough to describe the real energy distribution of each frequency component, and often gives false information especially in a short time window. [Mallat 2008]

However, this disadvanges can be solved by the continuous wavelet transform (CWT), which analyzes how the frequency content of a signal changes over time in a self-adaptive way. Wavelets can be localized in both time and frequency whereas the standard Fourier transform is only localized in frequency. Figure 14 shows how this earthquake signals are analyzed jointly in time and frequency. In the first P arrival, there is an apparent energy peak located near around 0.6Hz. This could also be an indication for how to choose time window. Some sliding fk analysis [Rost and Weber 2001] not considering

the time-varying frequency component would be less reliable.

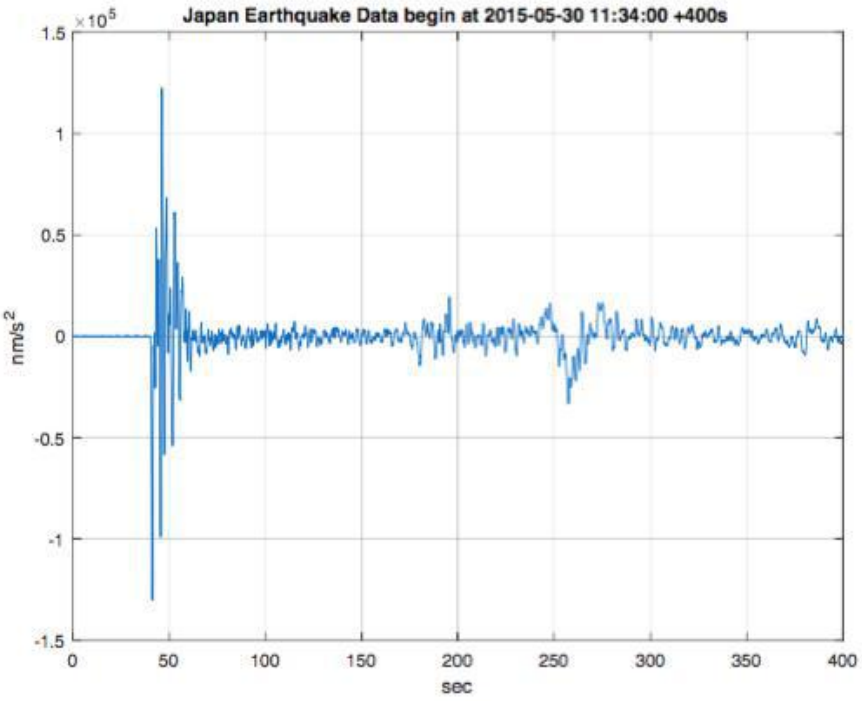

(a) Seismograph Data in the first 6 mins

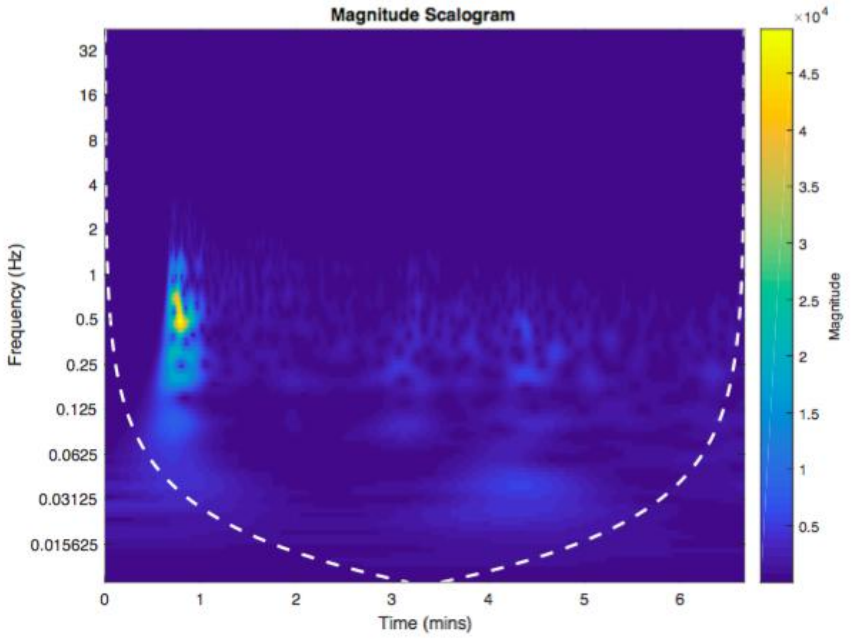

(b) CWT of the Seismograph Data in the first 6 mins

Figure 14. CWT of 2015 Japan Earthquake Data

4.2. Looking for similar scattering pattern

To better identify the shallow scattering, more evidence is needed. One possible way to illustrate this may is that we try to look for more earthquakes and see if we can find the

same or similar scattering patterns. This could be a strong evidence to imply the shallow scattering. We could cross-correlate different earthquake coda waves (early coda) to see if they have a higher cross-correlation coefficients or share some similar patterns.

5. Conclusion

(1) the "deep" stations (4000's) have a more coherent signal than the "shallow" stations (0-300), (2) station geometry have an influence on the shape of the fk peak, but roughness of the fk plot is due to the data, (3) higher frequency range we stack, the incoherent the fk plot looks, (4) limitation of the station number and distribution makes it hard to identify how the incoherence varies with space. This result seems to be consistent with near-surface scattering and potentially indicates that complexity decreases with depth.

6. Acknowledgments

The author thanks his mentor V. Tsai for his patient guidance. The author thanks L. Liberty, G. Gribler, T. Harper for their help in Boise. The author thanks D. Bowden, V. Lai, J. Muir, W. Liu, S. Huang for their helpful suggestions and discussions. The author thanks V. Mandic, G. Pavlis, D. Sun, H. Yao for their helpful comments. The research was supported by School of Earth and Space Science, USTC and Caltech Seismological Laboratory.

References

Aki, K. and Richards, P. G. (2002). *Quantitative seismology*, volume 1.

Harms, J., Sajeva, A., Trancynger, T., DeSalvo, R., Mandic, V., and Collaboration, L. S. (2009). Seismic studies at the homestake mine in lead, south dakota. *LIGO document*, pages T0900112–v1.

Mallat, S. (2008). *A wavelet tour of signal processing: the sparse way*. Academic press.

Park, C. B., Miller, R. D., and Xia, J. (1999). Multichannel analysis of surface waves. *Geophysics*, 64(3):800–808.

Rost, S. and Thomas, C. (2002). Array seismology: Methods and applications. *Reviews of geophysics*, 40(3).

Rost, S. and Weber, M. (2001). A reflector at 200 km depth beneath the northwest pacific. *Geophysical Journal International*, 147(1):12–28.

Sato, H., Fehler, M. C., and Maeda, T. (2012). *Seismic wave propagation and scattering in the heterogeneous earth*, volume 496. Springer.

Scherbaum, F., Gillard, D., and Deichmann, N. (1991). Slowness power spectrum analysis of the coda composition of two microearthquake clusters in northern switzerland. *Physics of the earth and planetary interiors*, 67(1):137–161.

Schuster, G. T. and Quintus-Bosz, A. (1993). Wavepath eikonal traveltime inversion: Theory. *Geophysics*, 58(9):1314–1323.

Shearer, P. M. (2007). Seismic scattering in the deep earth. *Treatise on geophysics*, 1:695–730.

Sheng, J., Leeds, A., Buddensiek, M., and Schuster, G. T. (2006). Early arrival waveform tomography on near-surface refraction data. *Geophysics*, 71(4):U47–U57.

Spudich, P. and Bostwick, T. (1987). Studies of the seismic coda using an earthquake cluster as a deeply buried seismograph array. *Journal of Geophysical Research: Solid Earth*, 92(B10):10526–10546.